Solid State Phenomena
ISSN: 1662-9779, Vol. 316, pp 928-935

Submitted: 2020-04-03
Accepted: 2020-05-29
Online: 2021-04-14

Determination Coefficient of Stress Concentration Using a Conformed Display on a Circle of a Single Radius

Alexander Shapoval[1,a], Iurii Savchenko[2,b], Oleg Markov[3,c*]

[1]Kremenchuk Mykhailo Ostrohradskyi National University, Kremenchuk, Ukraine

[2]Dnipropetrovsk State University of Internal Affairs, Dnipro, Ukraine

[3]Donbass State Engineering Academy, Kramatorsk, Ukraine

[a]alexshap.as@gmail.com, [b]savcheny@ua.fm, [c]oleg.markov.omd@gmail.com

Keywords: mathematical model, heterogeneous medium, defect formation, coefficient of stress concentration, conformal display on a circle of a single radius.

Abstract. Developed a mathematical model, which makes it possible to optimize, from the point of view of defect formation, the parameters of stress concentration in a deformable elastic body of the materials being processed, destruction is considered as a method for creating defects at a submicroscopic level in various media. Getting expressions of conformal reflection of single circle on an arbitrary area, using a conformal reflection and transformation of Laplace, it is possible to design behavior of a tensely deformed state of solid at the arbitrary loading.

Introduction

The problem of stress concentration in a deformable elastic body with various kinds of stress concentrators is in the field of attention of many researchers - mechanics, metallurgists, materials scientists. The relevance of this kind of research is determined by the applied nature of the problem. Regardless of what properties the composite will possess, the foreign phase is a stress concentrator in terms of strength. With the development of technological parameters of the impulse, I will pour on the special materials with the method of crushed the necessary protection against the regime, which allows us to delineate the product under the command of the authorities. [1]

Existing approaches towards research and workings in the area of explosion welding [2-4] are well defined along with the usage of shock-wave processing as a factor, which stimulates destruction of powder products of any configuration, with the end purpose of obtaining high quality powder for further formation, sintering and tool manufacturing of diverse application [5, 6]. Hard metal powder is used for manufacturing metallurgical and mechanical engineering tools. At present times, hard metal scrap is being exported outside Ukraine, and the Ukrainian manufacturers are importing tools. There is sufficient productive capacity within Ukraine itself for recycling scrap and manufacturing hard metal powder tools of guaranteed quality. The requirement of hard metal alloys is estimated at 600-700 tons per year. [7]

Amongst the ways to sort out the challenge may be shock-wave treatment, which ensures high pressure treatment and load speed of raw material as well as formation of high defect structure [8].

Regeneration oh hard metal alloys is performed through different chemo-thermal and metallurgical ways, amongst which are oxidation, carbonization and thermal treatment. However, these approaches show low productivity, are harmful for ecology and high in energy consumption.

Unlike classical mechanical-thermal approaches, which are limited in their physicochemical and mechanical effects, shock-wave treatment allows to make changes within the structure of material at all scale levels [9].

The need to assess the effect of shock waves of different intensity on the mechanism of defect formation and the process of destruction of a heterogeneous medium leads to theoretical studies [10-15].

The necessity of evaluating the effect of different shock waves strength onto the defects formation mechanism and the process of destruction of heterogeneous mediums has resulted in theoretical research. [16-19]

Goal of the research. To develop mathematical model of destruction of heterogeneous mediums, which will allow defining critical parameters of shock-wave treatment.

Materials and results of the research. Let's define the crack as a sinusoid $y=\sin\left(\frac{\pi}{2}+x\right)$, $x \in [a,b]$, where $[a,b]$ – segment or length of the investigated crack, points "a" and "b" – it's end coordinates according to Cartesian display XOY, with its start placed exactly in the middle of the positive semi-wave, which has a natural hole with maximum width of δ (Fig.1).

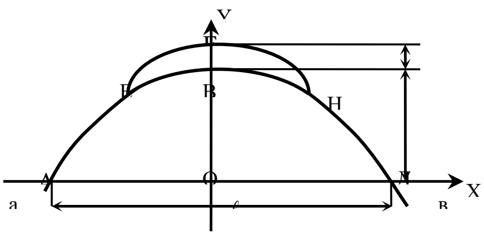

Fig. 1. Symmetrical crack-hole

To solve the problem, it is required to set 9 parameters: $\ell, \lambda, \delta, x_E, y_E, x_H, y_H, [a,b], n$. It is necessary to establish the equation of interpolating circles for top arch hole and bottom arch hole EFHB, ∪EFH and ∪ABD correspondingly. Let us find the equation of interpolating circle for the EFH arch. Referring to geometry course, we know that center of the circle lies at the intersection of perpendiculars, drawn from the medium of the EF and FH segments (pic. 2). Equation of the EF straight line, as the equation of the straight line, which passes through two points $E(x_E, y_E)$ and $F(O, \lambda+\delta)$ is

$$\begin{vmatrix} 0-x_E & \lambda+\delta-y_E \\ x-x_E & y-y_E \end{vmatrix} = 0 \tag{1}$$

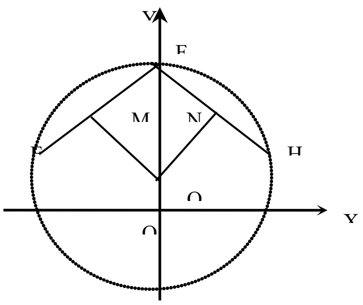

Fig. 2. Construction of interpolating circle for the EFH arch

The end equation of the EF straight line after transformation will look as follows

$$y = \frac{\lambda+\delta-y_E}{x_e} \cdot x + \lambda + \delta \tag{2}$$

Similarly, we arrive at the equation of the (FH) straight line

$$y = -\frac{\lambda+\delta-y_H}{x_H} x + \lambda + \delta \tag{3}$$

Coordinates of point M^1, as the medium of EF segment

$$x_{M^1} = \frac{x_E}{2},\ y_{M^1} = \frac{y_E+\lambda+\delta}{2} \tag{4}$$

Equation of the straight line (M^1O^{11}) shall be sorted as the equation of the perpendicular to the (EF) straight line intersecting at M^1, which can be transformed to

$$y = \frac{x_E}{\lambda + \delta - y_E} x + \frac{(\lambda + \delta)^2 - y_E^2 - x_E^2}{2(\lambda + \delta - y_E)} \tag{5}$$

Following same approach, we arrive at the equation of (N^1O^{11}) straight line

$$y = \frac{x_H}{\lambda + \delta - y_H} x + \frac{(\lambda + \delta)^2 - y_H^2 - x_H^2}{2(\lambda + \delta - y_H)} \tag{6}$$

Solving two equations (5) and (6), we shall find the coordinates of the center of the interpolating circle, point O^{11} ($X_O{}^{11}$, $Y_O{}^{11}$)

$$X_{O^{11}} = \frac{-\frac{(\lambda + \delta)^2 - x_E^2 - y_E^2}{2(\lambda + \delta - y_E)} + \frac{(\lambda + \delta)^2 - y_H^2 - x_H^2}{2(\lambda + \delta - y_H)}}{\frac{x_E}{\lambda + \delta - y_E} - \frac{x_H}{\lambda + \delta - y_H}} \quad , \tag{7}$$

$$Y_{O^{11}} = \frac{x_E}{\lambda + \delta - y_E} x_{O^{11}} + \frac{(\lambda + \delta)^2 - y_E^2 - x_E^2}{2(\lambda + \delta - y_E)}$$

Defining the radius of the interpolating circle r_2 as $|O^{11}F|$ distance

$$r_2 = |FO^{11}| = \sqrt{X_{O^{11}}^2 + (\lambda + \delta - Y_{O^{11}})^2} \tag{8}$$

Now we can write down the equation of interpolating circle Ω_2 for EFH arch

$$(X - X_{O^{11}})^2 + (Y - Y_{O^{11}})^2 = r_2^2 \tag{9}$$

To trace the ℓ parameter, we shall establish the interpolating circle outside ABD arch.
From the equations (9) and coordinates of $E(x_E, y_E)$ and $H(x_E, y_H)$ points.
Defining the angles tangent to these circles as well as their differences.
Let us define through

$$y_1 = Y_{O^1} + \sqrt{r_1^2 - (x - X_{O^1})^2} \; ; \tag{12}$$

$$y_2 = Y_{O^{11}} + \sqrt{r_2^2 - (x - X_{O^{11}})^2} \tag{13}$$

and find their derivatives at points E and H (fig. 3)

$$\left.\frac{dy_1}{dx}\right|_{x=x_E} = \frac{d}{dx}\left[Y_{O^1} + \sqrt{r_1^2 - (x - X_{O^1})^2}\right]_{x=x_E} = \frac{-x_E + X_{O^1}}{\sqrt{r_1^2 - (x_E - X_{O^1})^2}} \; ; \tag{14}$$

$$\left.\frac{dy_2}{dx}\right|_{x=x_E} = \frac{d}{dx}\left[Y_{O^{11}} + \sqrt{r_2^2 - (x - X_{O^{11}})^2}\right]_{x=x_E} = \frac{X_{O^{11}} - x_E}{\sqrt{r_2^2 - (x_E - X_{O^{11}})^2}} \; ; \tag{15}$$

Since functions derivatives in this point equal to tg of their tangents, this means that from (14) ÷ (15) we can obtain the values of $\varphi_Y, \theta_E, \varphi_H, \theta_H$ angles

$$\varphi_E = arctg\left(\frac{-x_E}{\sqrt{r_1^2 - x_E^2}}\right); \qquad \theta_E = arctg\left(\frac{X_{O^{11}} - x_E}{\sqrt{r_2^2 - \left(x_E - X_{O^{11}}\right)^2}}\right); \tag{16}$$

Let us take two complex planes: prototype plane Z and prototype plane W. Let us place our circular holler from problem 2 on the Z plane and reflect its surface onto the surface of the singular circle of W plane conforming it in few stages [20].

A broken line transformation

$$W_1 = \mathrm{A}_1 \frac{z' - z'_E}{z' - z'_H} \tag{17}$$

Realizes conforming reflection of the outer part of the circular holler onto the outer side of α_E angle. In fact, the top of α_E angle on the z' plane shifts to the point W_1=0 on the W_1 plane. By choosing complex constant A_1, it is possible to superpose one of the sides of α_E angle from W_1 plane with horizontal semi-axes.

Let us turn the angle into the upper semi-plane. This can be done through means of following transformation

$$W_2 = \sqrt[n]{W_1} \quad n = \frac{2\pi - \alpha_E}{\pi} \tag{18}$$

If $W_2 = \mathrm{B}_2 \exp(i\theta_2), W_1 = \mathrm{B}_1 \exp(i\theta_1),$ then considering (18) it follows, that $\mathrm{B}_2 = \mathrm{B}_1{}^{1/n}$, $\theta_2 = \dfrac{\theta_1}{n}$.

This way, the side of the angle $\theta_1 = 0$ superposes onto the current semi-axis on the W_2, plane, and the side $\theta_1 = (2\pi - \alpha_E)$ superposes to semi-straight line $\theta_2 = \pi.$

Combining transformations (17) and (18), we can conclude that function

$$W_2 = \sqrt{\mathrm{A}_1 \frac{z' - z'_E}{z' - z'_H}}\ . \tag{19}$$

Superposes outer part of the circular hole from plane Z onto the upper semi-plane W_2.

Let us look into the circle of the singular radius in the plane of complex variable W. Marking two pints on this circle $\mathrm{P}_E = \exp(i\psi_1)$ and $P_H = \exp(-i\psi_1)$.. The function realizes the reflection of the outer part of the singular radius circle onto the upper semi-plane.

$$W_2 = \mathrm{A}_2 \frac{W - \mathrm{P}_E}{W - \mathrm{P}_H} \tag{20}$$

Assuming $\mathrm{A}_2^{-1}\sqrt[n]{\mathrm{A}_1} = \mathrm{A},$ we can conclude that following transformation

$$\frac{W - P_E}{W - P_H} = \sqrt{\frac{z' - z'_E}{z' - z'_H}}\mathrm{A} \tag{21}$$

gives conforming reflection of outer part of the holler, placed on plane Z onto the outer part of the circle of the singular radius in the plane W.

Let us demand for point $z=\infty$ to superpose to point $W=\infty$, after which, considering (21) it follows that A = 1. This way, reflecting function for the circular holler type crack will be as follows

$$\frac{W-P_E}{W-P_H}=\sqrt{\frac{z'-z_E}{z'-z'_H}}\,. \tag{22}$$

Suppose $z'_E=r_2\exp(i\beta_E)$, $z'_H=r_2\exp(i\beta_H)$; $P_E=\exp(i\psi_E)$, $P_H=\exp(i\psi_H)$, and let point $z=r^2$ superpose during the reflection into the point $W=1$, then, considering (22) it follows that

$$\frac{1-\exp(i\psi_E)}{1-\exp(i\psi_H)}=\sqrt[n]{\frac{1-\exp(i\beta_E)}{1-\exp(i\beta_H)}}\,.$$

Where $\left[-\exp(i\psi_E)=\exp(i(\psi_E-\pi))\right]=\left[\sqrt{-\exp(i(\beta_E-\pi))}\right]$

and subsequently, $\psi_E-\pi=\dfrac{\beta_E-\pi}{n}$ (23)

and similarly $\psi_H-\pi=\dfrac{\beta_H-\pi}{n}$ (24)

From equation (22) we arrive to the final function of conforming reflection of the circular whole type crack surface into the singular radius circle

$$\frac{W-\exp(i\psi_E)}{W-\exp(i\psi_H)}=\sqrt{\frac{z'-z'_E}{z'-z'_H}} \tag{25}$$

Where

$$z'_E=x''_E+iy'_E,z'_H=x'_H+iy'_{H,}\ ,\ x'_E,x'_H\in\left[-\frac{\ell}{2}\cos\alpha_0+X_{O^{11}},\frac{\ell}{2}\cos\alpha_0+X_{O^{11}}\right],$$

$$y'_E,y'_H\in\left[Y_{O^{11}},(\lambda+\delta)\cos\alpha_0+Y_O{}^{11}\right].$$

We arrive at conforming transformations (25) as functions of two current coordinates *x*, *y* and seven parameters $\ell,\lambda,\delta,x_E,y_E,x_H,y_H$.

The expression of the conformal mapping of the unit circle on the considered area – a circular hole-like crack is equal to $z=\chi(W)$:

$$\chi(W)=\frac{z'_E\left(W-\exp(i\psi_H)\right)^{\frac{1}{n}}-z'_H\left(W-\exp(i\psi_E)\right)^{\frac{1}{n}}}{\left(W-\exp(i\psi_H)\right)^{\frac{1}{n}}-\left(W-\exp(i\psi_E)\right)^{\frac{1}{n}}}.\ \text{Where}\,|W|\le 1\,.$$

Points on the unit circle will be denoted by σ. According to $\exp(2i\dot{\gamma})=\dfrac{W^2}{\dot{r}^2}\dfrac{\chi'(W)}{\overline{\chi'(W)}}$ along the contour of the whole corresponding to the unit circle we have $\dfrac{d}{d\dot{S}}=\dfrac{1}{|\chi'(\sigma)|}\dfrac{d}{d\dot{\theta}}$.

When determining the stress concentration, it is found that the latter significantly depends on the curvature of the contour of the well $K=d\,\dot{\gamma}/d\dot{S}.:K=\dfrac{1}{|\chi'(\sigma)|}\left[1+\mathrm{Re}\left\{\dfrac{\sigma\chi''(\sigma)}{\chi'(\sigma)}\right\}\right]$

Thus, having obtained the expression of the conformal mapping of the unit circle onto an arbitrary region, using the conformal mapping and the Laplace transform, we can simulate the behavior of the stress-strain state of a solid body under arbitrary loads [21-24].

Analysis of the got dependences (Fig. 3), shows that at a permanent wave-length with the increase of amplitude the normal opening of banks diminishes, and a change increases and for every concrete crack aspires to some value. At identical amplitude with the increase of wave-length the normal opening and transversal change of banks increase.

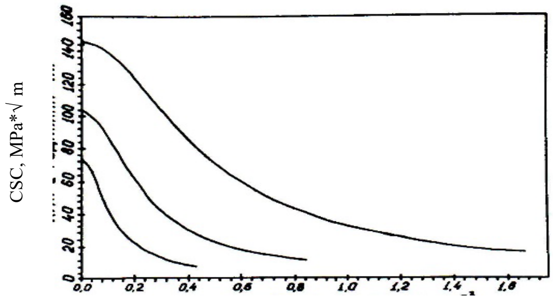

Fig. 3. Amplitude of wave, m*10^{-3}

Summary

Having obtained the expression of the conformal mapping of the unit circle onto an arbitrary region, using the conformal mapping and the Laplace transform, we can simulate the behavior of the stress-strain state of a solid body under arbitrary loads. There is a critical wave pressure for every material, exceeding which may lead to defects formation. Increase of system heterogeneity leads to the decrease of shock wave critical pressure, resulting in formation of defects and destruction of material. A mathematical model, which allows optimizing load parameters of the processed materials considering defects formation, was developed. Getting expressions of conformal reflection of single circle on an arbitrary area, using a conformal reflection and transformation of Laplace, it is possible to design behavior of the tensely deformed state of solid at the arbitrary loading.

References

[1] A. Anishchenko, V. Kukhar, V. Artiukh, O. Arkhipova. (2018). Application of G. Lame's and J. Gielis' formulas for description of shells superplastic forming, MATEC Web of Conferences, 2018, Vol. 238, pp. 06007(13 p.).

[2] Markov, O., Gerasimenko, O., Aliieva, L., Shapoval, A., Kosilov, M. Development of a new process for expanding stepped tapered rings (2019) Eastern-European Journal of Enterprise Technologies, 2 (1-98), pp. 39-46.

[3] Dragobetskii, V., Zagirnyak, V., Shlyk, S., Shapoval, A., Naumova, O. Application of explosion treatment methods for production items of powder materials [Zastosowanie metod eksplozyjnych do produkcji sproszkowanych materiałów] (2019) Przeglad Elektrotechniczny, 95 (5), pp. 39-42.

[4] D.B. Efremov, A.A. Gerasimova, S.M. Gorbatyuk, N.A. Chichenev. Study of kinematics of elastic-plastic deformation for hollow steel shapes used in energy absorption devices. CIS Iron and Steel Review, Vol. 18 (2019), pp. 30–34

[5] Gorbatyuk, S.M., Morozova, I.G., Naumova, M.G. Development of the working model of production reindustrialization of die steel heat treatment (2017) Izvestiya Ferrous Metallurgy, 60 (5), pp. 410-415.

[6] Babak, V.P., Shchepetov, V.V., Nedaiborshch, S.D. Wear resistance of nanocomposite coatings with dry lubricant under vacuum (2016) Naukovyi Visnyk Natsionalnoho Hirnychoho Universytetu, (1), pp. 47-52.

[7] Markov, O., Gerasimenko, O., Aliieva, L., Shapoval, A. Development of the metal rheology model of high-temperature deformation for modeling by finite element method (2019) EUREKA, Physics and Engineering, 2019 (2), pp. 52-60.

[8] Eron'ko, S.P., Gorbatyuk, S.M., Oshovskaya, E.V., Starodubtsev, B.I. Development of automatic system of gas-dynamic cut-off of slag for converter with rotating vessel shell (2017) Izvestiya Ferrous Metallurgy, 60 (11), pp. 863-869.

[9] Barabash A.V., Gavril'chenko E.Yu., Gribkov E.P., Markov O.E. (2014) Straightening of Sheet with Correction of Waviness. Steel in Translation 44,1:916–920.

[10] Gorbatyuk, S.M., Morozova, I.G., Naumova, M.G. Color Mark Formation on a Metal Surface by a Highly Concentrated Energy Source (2016) Metallurgist, 60 (5-6), pp. 646-650.

[11] G. Diachenko, O. Aziukovskyi, M. Rogoza and S. Yakimets, "Optimal Field-Oriented Control of an Induction Motor for Loss Minimization in Dynamic Operation," 2019 IEEE International Conference on Modern Electrical and Energy Systems (MEES), Kremenchuk, Ukraine, 2019, pp. 94-97.

[12] V. Kukhar, E. Balalayeva, A. Prysiazhnyi, O. Vasylevskyi, I. Marchenko. (2018). Analysis of relation between edging ratio and deformation work done in pre-forming of workpiece by bulk buckling, MATEC Web of Conferences, 2018, Vol. 178, pp. 02003 (6 p.).

[13] Zakharov, A.N., Gorbatyuk, S.M., Borisevich, V.G. Modernizing a press for making refractories (2008) Metallurgist, 52 (7-8), pp. 420-423.

[14] I. Lutsenko, E. Fomovskaya, S. Koval, O. Serdiuk. "Development of the method of quasioptimal robust control for periodic operational processes", Eastern-European Journal of Enterprise Technologies, vol. 4, no. 2-88, pp. 52−60, 2017.

[15] Shapoval A.N., Shapoval A.A. (2002) Development of The Unit for Multi-Stage Vibration Drawing of Metal Product. Tsvetnye Metally 4:77-82

[16] Gorbatyuk, S.M., Kochanov, A.V. Method and equipment for mechanically strengthening the surface of rolling-mill rolls (2012) Metallurgist, 56 (3-4), pp. 279-283.

[17] Radyuk, A.G., Gorbatyuk, S.M., Gerasimova, A.A. Use of electric-arc metallization to recondition the working surfaces of the narrow walls of thick-walled slab molds (2011) Metallurgist, 55 (5-6), pp. 419-423.

[18] Gorbatyuk, S.M., Pavlov, V.M., Shapoval, A.N., Gorbatyuk, M.S. Experimental use of rotary rolling mills to deform compacts of refractory metals (1998) Metallurgist, 42 (5-6), pp. 178-183.

[19] A. Anishchenko, V. Kukhar, V. Artiukh, O. Arkhipova. (2018). Superplastic forming of shells from sheet blanks with thermally unstable coatings, MATEC Web of Conferences, 2018, Vol. 238, pp. 06006 (6 p.).

[20] Markov, O.E., Gerasimenko, O.V., Shapoval, A.A., Abdulov, O.R., Zhytnikov, R.U. Computerized simulation of shortened ingots with a controlled crystallization for manufacturing of high-quality forgings (2019) International Journal of Advanced Manufacturing Technology, 103 (5-8), pp. 3057-3065.

[21] Dragobetskii V., Zagirnyak M., Naumova O., Shlyk S., Shapoval A. (2018) Method of determination of technological durability of plastically deformed sheet parts of vehicles. International Journal of Engineering and Technology(UAE) 7,4,:92-99.

[22] Moroz, M., Korol, S., Chernenko, S., Boiko, Y., Vasylkovskyi, O. Driven camshaft power mechanism of the vehicle diesel engine fuel pump (2018) International Journal of Engineering and Technology(UAE), 7 (4), pp. 135-139. DOI: 10.14419/ijet.v7i4.3.19723

[23] I. Lutsenko, E. Fomovskaya, I. Oksanych, S. Koval, O., Serdiuk. “Development of a verification method of estimated indicators for their use as an optimization criterion”, Eastern-European Journal of Enterprise Technologies, vol. 2, no. 486, pp. 17−23, 2017

[24] M. Zagirnyak, V. Zagirnyak, D. Moloshtan, V. Drahobetskyi, A. Shapoval (2019) A search for technologies implementing a high fighting efficiency of the multilayered elements of military equipment Eastern-European Journal of Enterprise Technologies, 6/1 (102), P 33-40.